

# Analytical and Monte-Carlo modeling of Multi-Parallel Slit and Knife-Edge Slit Prompt Gamma Cameras

E. Testa<sup>1</sup>, B.F.B. Huisman<sup>1,2</sup>, D. Dauvergne<sup>3</sup>, J. M. Létang<sup>2</sup>, D. Sarrut<sup>3</sup>

<sup>1</sup>Université de Lyon, Université Claude Bernard Lyon 1, CNRS/IN2P3, Institut de Physique Nucléaire de Lyon, 69622 Villeurbanne, France,  
<sup>2</sup>CREATIS, Université de Lyon; CNRS UMR5220; INSERM U1044; INSA-Lyon; Université Lyon 1; Centre Léon Bérard, Lyon, France, <sup>3</sup>Université Grenoble Alpes, Laboratoire de Physique Subatomique et de Cosmologie, CNRS/IN2P3, Grenoble, France

## Introduction

### Ion-range verification during hadrontherapy

- Major challenge to fully take benefit from ion beam ballistic properties
- Main imaging modalities under study: prompt gammas (PG) detection [1] with non-imaging systems (such as PG Timing, PG Spectroscopy and PG Peak Integral) and imaging systems, namely physically-collimated or electronically collimated cameras (Compton cameras)

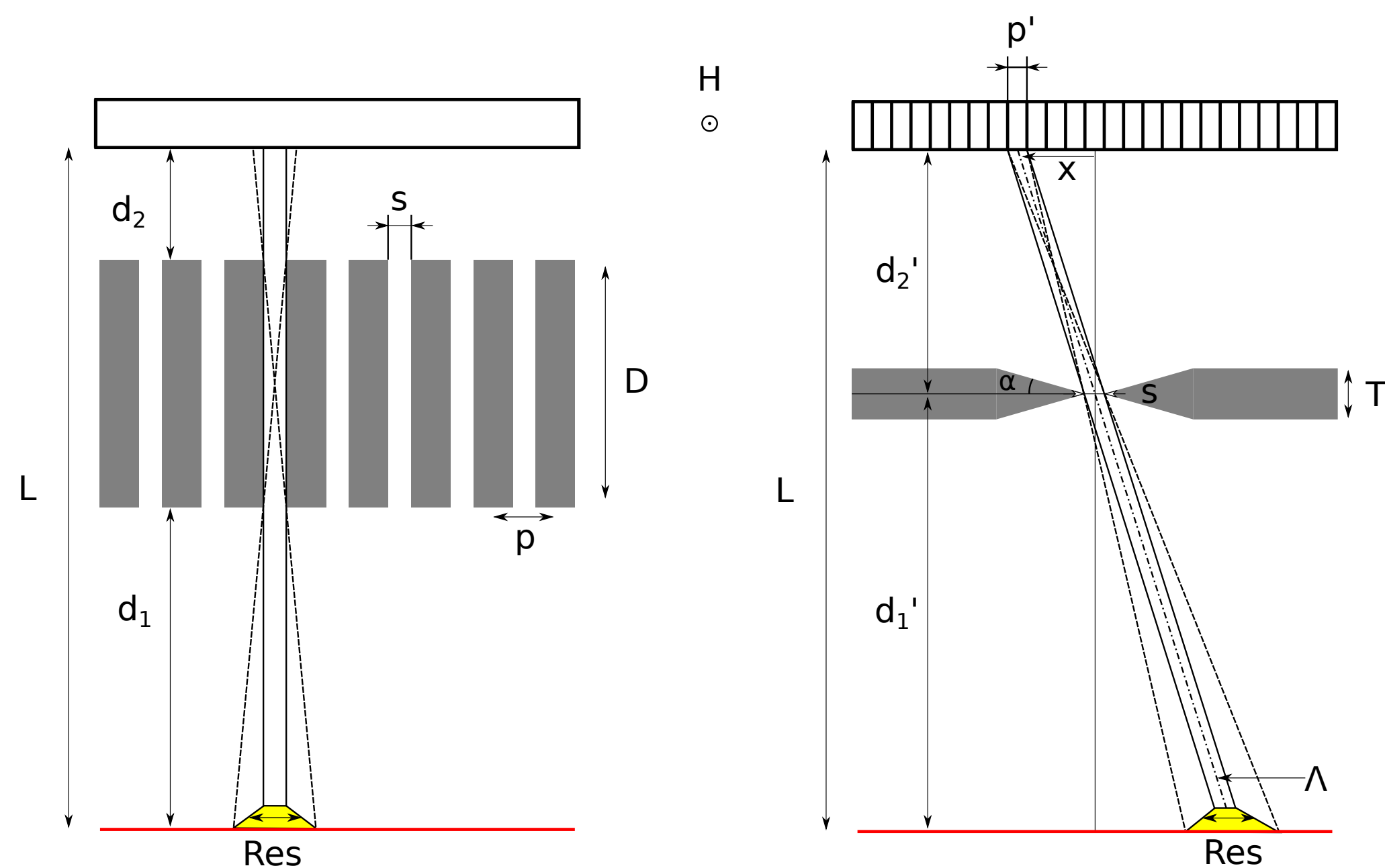
### PG collimated cameras

- 2 main collimator configurations: Multi-Parallel Slit (MPS) [2] and Knife-Edge Slit (KES) collimators [3] (Figure XXX)
- No theoretical considerations have been proposed for the specific 1D collimation systems developed for PG detection

## Objectives

- Development an analytical model (AM) of MPS and KES collimations  $\Rightarrow$  main intrinsic features of each collimator
- Verification of the AM by means of Monte Carlo (MC) simulations
- Comparison the two MPS and KES prototypes developed by IBA and the CLaRyS collaboration, respectively.

## The Analytical Model of MPS and KES collimations



	MPS	KES
Effective slit width ( $s_e$ )	$s$	$s + \frac{\ln(2)}{\mu \tan(\alpha)}$
Spatial resolution (Res)	$s \left(1 + \frac{d_1}{D}\right)$	$s_e \left(1 + \frac{d_1'}{d_2'}\right)$
Detection efficiency (Eff)	$\frac{Hs}{4\pi LD}(1-f)$	$\frac{Hs_e}{4\pi Ld_2'} \left(1 + \frac{x^2}{d_2'^2}\right)^{-3/2}$
Collimator effective thickness ( $T_e$ )	$D \times f$	$T$

Table 1: Detection efficiencies and spatial resolution predicted by the analytical model

## Monte Carlo simulations

- Gate 7.2 with Geant4 4.10.02 and the QGSP\_BIC\_HP\_EMY physics list
- Optimization: vpgTLE variance reduction method  $\Rightarrow$  gain of  $\sim 10^3$  [4]
- Background (BKG) modeling:
  - Estimates of background counts in the detector are taken from [5] (KES,  $2.5 \cdot 10^{-7}$  counts/incident proton and per 8 mm bin) and [2] (MPS,  $5 \cdot 10^{-7}$  counts per primary proton per 4 mm bin) which are both based on measured data

## Figures of merit

- Detection efficiency: #detected PG/#emitted PG in the camera Field of View (FOV)
- Spatial resolution: the width of the PG profile fall-off, namely the FWHM of the peak resulting from the computation of the PG profile first derivative
- Fall-off Retrieval Precision (FRP): **TODO**

## References

- [1] J. Krimmer and et al., "Prompt-gamma monitoring in hadrontherapy: A review," *NIMA*, 2017.
- [2] M. Pinto and et al., "Design optimisation of a TOF-based collimated camera prototype for online hadrontherapy monitoring," *PMB*, vol. 59, 2014.
- [3] J. Smeets and et al., "Prompt gamma imaging with a slit camera for real-time range control in proton therapy," *PMB*, 2012.
- [4] B. F. B. Huisman and et al., "Accelerated prompt gamma estimation for clinical proton therapy simulations," *PMB*, 2016.
- [5] I. Perali and et al., "Prompt gamma imaging of proton pencil beams at clinical dose rate," *PMB*, 2014.

## Simulated geometries

- 2 configurations (Table 2):
  - The prototypes as they are published (Figure 1)
  - The prototypes with some alterations for the Analytical Model Verification (AMV), in particular the use of "perfect" collimators and detectors (full gamma absorption)

	AMV	PC
Absorber	MPS KES	BGO LYSO
Energy selection	MPS KES	$> 1$ MeV 3–6 MeV
TOF selection	MPS KES	TOF no TOF
BKG	No modeling	Exp. data based
Target	No	Yes
Beam	160 MeV proton	

Table 2: AMV: Analytical Model Verification – PC: Prototypes Comparison. For AMV, the PG source corresponds to the PG emitted along the beam direction during the PMMA irradiation

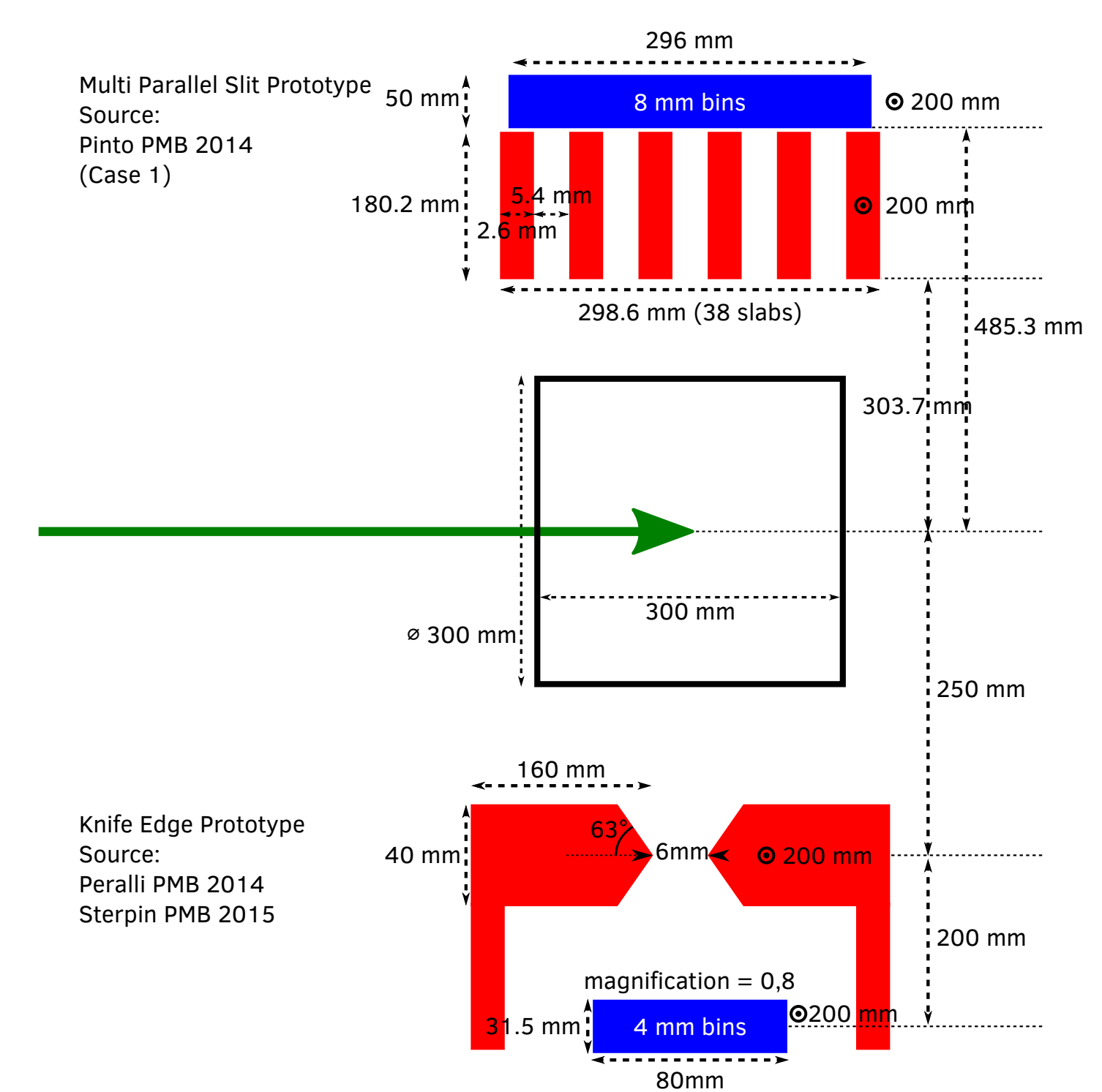


Figure 1: Change the target diameter: 15 cm

## Results

### AMV

	MPS		KES	
	AM	MC	AM	MC
Res	14.52 mm	17.9 mm	13.5 mm	13.8 mm
Eff	$6.66 \cdot 10^{-4}$	<b>TODO</b>	$1.06 \cdot 10^{-3}$	<b>TODO</b>

### PG profiles detected by the prototypes

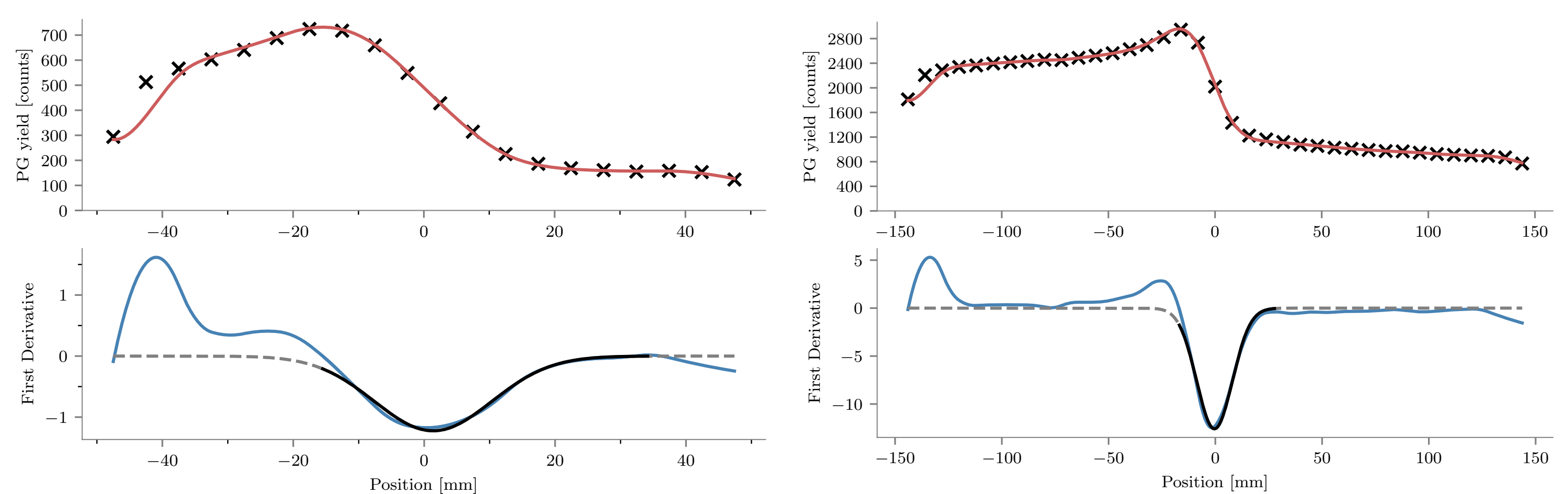


Figure 2: PG profiles: MPS (left), KES (right). See Table 2 for the parameters.

### Fall-off Retrieval Precision

Time selection	ToF				None			
	$> 1$		3–6		$> 1$		3–6	
Energy selection (MeV)								
Camera	MPS	KES	MPS	KES	MPS	KES	MPS	KES
$10^9$ (# protons)	<b>0.37</b>	0.55	0.44	1.07	0.42	0.74	0.66	<b>1.32</b>
$10^8$	<b>1.35</b>	2.08	1.60	4.22	1.36	1.82	2.00	<b>9.70</b>
$10^7$	<b>4.41</b>	11.88	20.36	20.50	22.45	17.18	56.92	<b>19.39</b>

Table 3: **TO VERIFY: Standard deviation of the FOP distribution.** In bold, the cuts and ToF selections as proposed.

## Acknowledgments



This work is supported by the Labex PRIMES ANR-11-LABX-0063.